

# Targeting of tumor growth and angiogenesis underlies the enhanced antitumor activity of lenvatinib in combination with everolimus

Masahiro Matsuki, Yusuke Adachi, Yoichi Ozawa, Takayuki Kimura, Taisuke Hoshi, Kiyoshi Okamoto,<sup>1</sup> Osamu Tohyama,<sup>1</sup> Kaoru Mitsuhashi, Atsumi Yamaguchi, Junji Matsui and Yasuhiro Funahashi

Tsukuba Research Laboratories, Eisai Co., Ltd., Tsukuba, Ibaraki, Japan

## Key words

Combination, everolimus, fibroblast growth factor, lenvatinib, renal cell carcinoma

## Correspondence

Yasuhiro Funahashi, Tsukuba Research Laboratories, Eisai Co., Ltd., 5-1-3 Tokodai, Tsukuba, Ibaraki 300-2635, Japan.  
Tel: +81-29-847-5615; Fax: +81-29-847-7614;  
E-mail: y-funahashi@hhc.eisai.co.jp

<sup>1</sup>Present address: Eisai Co., Ltd., Tokyo, Japan

## Funding Information

This research was funded by Eisai Co., Ltd.

Received September 22, 2016; Revised January 6, 2017;  
Accepted January 7, 2017

*Cancer Sci* 108 (2017) 763–771

doi: 10.1111/cas.13169

The combination of lenvatinib, a multiple receptor tyrosine kinase inhibitor, plus everolimus, a mammalian target of rapamycin (mTOR) inhibitor, significantly improved clinical outcomes versus everolimus monotherapy in a phase II clinical study of metastatic renal cell carcinoma (RCC). We investigated potential mechanisms underlying the antitumor activity of the combination treatment in preclinical RCC models. Lenvatinib plus everolimus showed greater antitumor activity than either monotherapy in three human RCC xenograft mouse models (A-498, Caki-1, and Caki-2). In particular, the combination led to tumor regression in the A-498 and Caki-1 models. In the A-498 model, everolimus showed antiproliferative activity, whereas lenvatinib showed anti-angiogenic effects. The anti-angiogenic activity was potentiated by the lenvatinib plus everolimus combination in Caki-1 xenografts, in which fibroblast growth factor (FGF)-driven angiogenesis may contribute to tumor growth. The combination showed mostly additive activity in vascular endothelial growth factor (VEGF)-activated, and synergistic activity against FGF-activated endothelial cells, in cell proliferation and tube formation assays, as well as strongly suppressed mTOR-S6K-S6 signaling. Enhanced antitumor activities of the combination versus each monotherapy were also observed in mice bearing human pancreatic KP-1 xenografts overexpressing VEGF or FGF. Our results indicated that simultaneous targeting of tumor cell growth and angiogenesis by lenvatinib plus everolimus resulted in enhanced antitumor activity. The enhanced inhibition of both VEGF and FGF signaling pathways by the combination underlies its superior anti-angiogenic activity in human RCC xenograft models.

Lenvatinib mesilate (lenvatinib) is an orally administered, multitargeted tyrosine kinase inhibitor that selectively inhibits VEGFR1–3, FGFR1–4, platelet-derived growth factor receptor  $\alpha$ , RET, and KIT. In 2015, lenvatinib was approved in the USA, the EU, and Japan for the treatment of progressive, locally recurrent or metastatic, radioactive iodine-refractory differentiated thyroid cancer, or unresectable thyroid cancer.<sup>(1)</sup> Lenvatinib blocks VEGF- and FGF-driven angiogenesis, KIT-dependent angiogenesis, RET-fusion/Ret mutant tumorigenesis, and VEGFR3-associated lymphangiogenesis.<sup>(2–6)</sup> Phase I clinical trials have shown the activity of lenvatinib against multiple types of cancer,<sup>(7,8)</sup> and several phase II/III trials of lenvatinib as a monotherapy or in combination with other drugs are ongoing.

Renal cell carcinoma is the most common type of kidney cancer and approximately 30% of patients have metastatic disease at the time of diagnosis.<sup>(9,10)</sup> In clear-cell RCC, the most prominent subtype of RCC, the VHL tumor-suppressor protein is frequently inactivated, leading to the activation of HIF and consequent upregulation of the proangiogenic factor VEGF.<sup>(11–15)</sup> Due to this characteristic of RCC, the standard of care for first-line treatment of patients with advanced or mRCC

includes VEGF or VEGFR-targeted anti-angiogenic therapeutics.<sup>(16)</sup> In addition, the mTOR pathway is also activated in RCC.<sup>(17,18)</sup> In preclinical models, treatment with everolimus, an mTOR inhibitor, had direct antitumor effects through cell cycle arrest and increased apoptosis, as well as anti-angiogenic activity.<sup>(19,20)</sup> Everolimus was approved and has been used as a second-line therapy for the treatment of advanced RCC.<sup>(16)</sup>

Despite the improvements in patient outcomes with these targeted therapies for mRCC, the 5-year relative survival of patients with mRCC remains low,<sup>(21)</sup> indicating that improved therapeutic strategies in this setting are still required. One possible treatment strategy is the combination of two classes of targeted agents, namely VEGF-targeted agents and mTOR inhibitors. Indeed, this combination has been investigated in a number of clinical studies of mRCC; however, almost all of these trials have yielded disappointing outcomes due to unacceptable safety profiles and/or poor efficacy.<sup>(22)</sup> In a recent phase II clinical study of patients with mRCC who had progressed on a VEGFR-targeted therapy, lenvatinib in combination with everolimus significantly improved clinical outcomes compared with everolimus monotherapy (NCT01136733),<sup>(23)</sup>

and this combination treatment was approved in the USA and EU in 2016. However, the detailed mechanisms underlying the efficacy of this combination treatment remain to be elucidated.

Here, we investigated the mechanism underlying the efficacy of the lenvatinib plus everolimus combination in preclinical models. Our study showed that the ability of the combination to both inhibit angiogenesis and exert direct antitumor effects led to tumor xenograft regression. In addition, our data showed simultaneous targeting of VEGFR/FGFR and the downstream mTOR pathway in endothelial cells by the lenvatinib plus everolimus combination potentially enhanced the anti-angiogenic phenotypes of the individual agents.

## Materials and Methods

**Cell lines and reagents.** All RCC cell lines were obtained from the ATCC (Manassas, VA, USA). A-498 cells were cultured in RPMI-1640 supplemented with 10% FBS and p/s. Caki-1 and Caki-2 cells were cultured in RPMI-1640 supplemented with 10% FBS, 1 mmol/L sodium pyruvate, 50 μmol/L 2-mercaptoethanol, and p/s. KP-1 transfectants overexpressing either human VEGF121 (KP-1/VEGF) or mouse FGF4 (KP-1/FGF) were established previously,<sup>(6)</sup> and were cultured in RPMI-1640 supplemented with 10% FBS, 0.6 mg/mL Geneticin (Wako, Osaka, Japan), sodium pyruvate, 2-mercaptoethanol, and p/s. Human umbilical vein endothelial cells were isolated from a human umbilical cord that was obtained with informed consent in the Shoji clinic (Tsukuba, Japan). The experiments using the umbilical cord and isolated HUVECs were approved by the Research Ethics Committee of Eisai Co., Ltd. The HUVECs were maintained in EGM-2 BulletKit (Lonza, Basel, Switzerland) and used at passage 3 or 4. All cells were maintained at 37°C in 5% CO<sub>2</sub>. Lenvatinib and PD173074 were synthesized at Eisai Co., Ltd. (Tsukuba, Japan). Everolimus was purchased from LC Laboratories (Woburn, MA, USA).

**Western blot analysis.** The HUVECs were seeded at  $3 \times 10^5$  cells/dish in 60-mm dishes, cultured overnight, and then starved in Human Endothelial-SFM (Life Technologies, Carlsbad, CA, USA) with 0.5% FBS and p/s for approximately 16 h. The cells were treated for 1 h with vehicle only or lenvatinib, everolimus, or both, then stimulated with 20 ng/mL VEGF (R&D Systems, Minneapolis, MN, USA) or 20 ng/mL bFGF (Invitrogen, Carlsbad, CA, USA) for 30 min. The cells were then rinsed with PBS

and lysed with RIPA buffer (Thermo Fisher Scientific, Waltham, MA, USA) containing protease inhibitor cocktail (Roche Diagnostics, Mannheim, Germany) and phosphatase inhibitor cocktail 2 and 3 (Sigma-Aldrich, St. Louis, MO, USA). Cell lysates were sonicated and centrifuged at 21 600 g for 20 min at 4°C. Lysed samples were electrophoresed in 5%–20% polyacrylamide gels. Separated proteins were transferred onto PVDF membranes. The membranes were blocked with 5% skim milk or BSA dissolved in Tris-buffered saline (Takara Bio, Shiga, Japan) with 0.1% Tween 20 and incubated individually with the following primary antibodies: Erk1/2, pErk1/2, S6K, pS6K (T389), pS6K (T421/S424), S6, pS6 (S235/S236) (Cell Signaling Technology, Beverly, MA, USA), and β-actin (Sigma-Aldrich). All the primary antibodies were diluted 1:2000, except β-actin, which was diluted 1:10 000. Each membrane was then washed and incubated with HRP-conjugated secondary antibody (1:5000; Cell Signaling Technology), and antibody complexes were detected with the ECL Prime Western Blotting Detection System (GE Healthcare Life Sciences, Little Chalfont, UK). Immunoreactive bands were visualized using an image analyzer (LAS-4000; Fuji Film, Tokyo, Japan).

**Human umbilical vascular endothelial cell proliferation assay.** The HUVECs were seeded at  $1.5 \times 10^3$  cells/well in 96-well plates in Human Endothelial-SFM supplemented with 2% FBS and p/s, and cultured overnight. The cells then were treated with vehicle only (control) or 1:2 serial dilutions of lenvatinib, everolimus, or both at the fixed dose ratios indicated in Table 1 in the presence of 5 ng/mL VEGF (R&D Systems) and cultured for 3 days. Cell viability was determined using a Cell Counting Kit-8 (Dojindo Molecular Technologies, Kumamoto, Japan). The optical density at 450 nm (reference, 650 nm) of each well was measured by using a microplate reader (SpectraMax 250; Molecular Devices, Sunnyvale, CA, USA). Inhibition of cell growth (fractional inhibition) was determined, and the resulting values were used to calculate the CI. Each experiment contained triplicate samples, and two independent experiments were carried out.

**Tube formation assay.** Geltrex (Life Technologies) was added to 96-well plates at 45 μL/well and incubated at 37°C for 1 h. The HUVECs were diluted in Medium 200PRF (Life Technologies) and seeded on the gel at  $1.2 \times 10^4$  cells/well. The cells were treated with vehicle only (control) or 1:2 serial dilutions of lenvatinib, everolimus, or both at the fixed dose ratios indicated in Table 1 in the presence of 20 ng/mL bFGF (Invitrogen) and

**Table 1.** Effects of lenvatinib plus everolimus on vascular endothelial growth factor (VEGF)-induced proliferation and basic fibroblast growth factor (bFGF)-induced tube formation of HUVECs

Drug	Lenvatinib / everolimus ratio	IC <sub>50</sub> of lenvatinib, nmol/L	IC <sub>50</sub> of everolimus, nmol/L	CI† at IC <sub>50</sub>	Combination effect‡
<b>(a) VEGF-induced proliferation</b>					
Lenvatinib	–	2.10	–	–	–
Everolimus	–	–	0.69	–	–
Combination	2.5:1	0.75	0.30	0.80	Moderate synergism
	5:1	1.44	0.29	1.11	Additive
	10:1	1.79	0.18	1.12	Additive
	20:1	2.12	0.11	1.17	Additive
<b>(b) bFGF-induced tube formation</b>					
Lenvatinib	–	30.3	–	–	–
Everolimus	–	–	75.0	–	–
Combination	1:4	5.43	21.7	0.47	Synergism
	1:8	4.00	32.0	0.56	Synergism
	1:12	3.17	38.0	0.61	Synergism
	1:16	3.01	48.1	0.74	Moderate synergism

Data are presented as geometric means of two independent experiments performed in triplicate. †Combination index (CI) was calculated using CalcuSyn software. ‡Combination effects were evaluated as described in Materials and Methods. –, Not applicable.

cultured for 22 h at 37°C in 5% CO<sub>2</sub>. After the incubation, MTT was added to each well, and the cells were incubated for a further 2 h. Images of capillary-like structures were obtained (Gel-Count; Oxford Optronix, Abingdon, UK), and tube length was measured (In Cell Developer Toolbox, version 1.9.2; GE Healthcare). Inhibition of tube formation (fractional inhibition) was determined, and the resulting values were used to calculate the CI. Each experiment included triplicate samples, and two independent experiments were carried out.

**Determination of the combination index.** The effects of the drug combinations were evaluated according to the median-effect equation.<sup>(24,25)</sup> The fractional inhibition values were imported into CalcuSyn software (version 2.0; Biosoft, Cambridge, UK) to determine the median-effect dose ( $D_m$ , equivalent to the IC<sub>50</sub> value), and the CI values at the IC<sub>50</sub>. According to previously reported definitions of synergism or antagonism,<sup>(25)</sup> the following CI ranges were applied: synergism,  $CI \leq 0.7$ ; moderate synergism,  $0.7 < CI \leq 0.85$ ; additive effect,  $0.85 < CI \leq 1.2$ ; moderate antagonism,  $1.2 < CI \leq 1.45$ ; and antagonism,  $1.45 < CI$ .<sup>(25)</sup> Of note, the linearity of median-effect plots for some monotherapies was compromised because the maximum effects did not achieve complete inhibition. In those cases, fractional inhibition values of  $\leq 0.5$  and the lowest value exceeding 0.5 for each treatment were used for CI determination to avoid overestimation of the effect.

**Renal cell carcinoma cell line proliferation assay.** A-498 and Caki-1 cells were plated on 96-well plates at 100 cells/well, cultured overnight, treated with vehicle only (control) or 1:3 serial dilutions of lenvatinib or everolimus, and then cultured. On day 3 after the addition of these drugs or vehicle, the medium was replaced with freshly prepared drug (or vehicle)-containing medium, and the cells were incubated for another 3 days. Cell viability was determined by using a Cell Counting Kit-8, and IC<sub>50</sub> values were calculated by using GraphPad Prism 6.05 (GraphPad Software, La Jolla, CA, USA). Each experiment contained triplicate samples, and three independent experiments were carried out.

**Human cancer cell xenograft mouse models.** Animal experiments were carried out in accordance with the Institutional Animal Care and Use Committee guidelines of Eisai Co., Ltd. Female BALB/c nude mice (CAnN.Cg-Foxn1<sup>nu</sup>/CrIj) were obtained from Charles River Laboratories Japan (Kanagawa, Japan). A-498, Caki-1, and Caki-2 cells were suspended in 50% Matrigel (Corning, Corning, NY, USA) and KP-1 transfectants were suspended in Geneticin-free medium at  $5 \times 10^7$ – $1 \times 10^8$  cells/mL; 0.1–0.2 mL cell suspension was inoculated s.c. into the right flank of each mouse. Once the tumors had reached the desired volume, the mice were selected according to tumor volume and shape and randomly allocated to treatment groups (day 1). Lenvatinib was dissolved in 3 mmol/L HCl or distilled water. Everolimus was dissolved in a solution comprising DMSO, Tween-80, and 5% glucose (35:65:900 [or 1:2:27]), and PD173074 was dissolved in distilled water containing equimolar HCl. Each diluted drug or vehicle was given orally to individual mice once daily. Tumor dimensions were measured twice weekly with a caliper, and tumor volume was calculated as  $\frac{1}{2} \times \text{length} \times \text{width}^2$ . The RTV was calculated by dividing the daily tumor volume by that of the same mouse on day 1. Body weight was also measured twice weekly, and the relative body weight was calculated by dividing the daily body weight by that of the same mouse on day 1.

**Measurement of microvessel density.** Fragments of resected tumor xenografts were fixed with 10% formalin and embedded in paraffin. Tissue sections were stained with rat anti-mouse CD31 mAb (1:100; clone SZ31, Dianova) and visualized using a Vectastain Elite ABC kit (Vector Laboratories, Burlingame, CA, USA)

or DAB MAP kit (Roche Diagnostics). Nuclei were counterstained with hematoxylin. The slides were scanned using the ScanScope XT system (Aperio; Leica Biosystems, Wetzlar, Germany); the five regions of interest (each 500 × 500 μm) with the highest densities of CD31-stained microvessels in each tumor slice were selected manually (ImageScope v.12.1.0.5029; Leica Biosystems). The number of microvessels in each region of interest was measured using the Microvessel Analysis Algorithm v1.0 (Leica Biosystems). Microvessel density was expressed as the number of microvessels per mm<sup>2</sup>; the mean MVD of the five regions of interest was defined as the MVD of the tumor.

**Statistical analysis.** Antitumor and anti-angiogenic activities were compared between treatment groups using the Dunnett multiple comparison test. Comparisons between two groups were by unpaired *t*-test. A *P*-value of  $<0.05$  was defined as significant. Statistical analyses were carried out using GraphPad Prism 6.05 software.

Additional Materials and Methods are provided in Appendix S1 and Table S1.

## Results

**Antitumor activity of the combination of lenvatinib plus everolimus in human RCC xenograft mouse models.** We first evaluated the antitumor activity of lenvatinib and everolimus as monotherapies and in combination in three human RCC xenograft (A-498, Caki-1, and Caki-2) mouse models. The RCC cells were s.c. inoculated, and when tumor sizes had reached 200–350 mm<sup>3</sup> (day 1), the mice were randomly allocated into four groups for each xenograft model. Mice then received vehicle only, lenvatinib at 10 mg/kg, everolimus at 30 mg/kg, or the combination of lenvatinib (10 mg/kg) plus everolimus (30 mg/kg) orally daily for 14 days. In all three RCC xenograft models tested, each monotherapy showed inhibition of tumor growth on day 15 compared with vehicle only control (Fig. 1a). Combination treatment with lenvatinib plus everolimus yielded significantly greater inhibition of tumor growth compared with each monotherapy in all three models (Fig. 1a) and led to tumor regression in the A-498 and Caki-1 models (Fig. 1a). The combination treatment was well tolerated and did not cause increased loss of body weight compared with that observed with lenvatinib or everolimus monotherapy (Fig. 1b).

**Anti-angiogenic activity of the combination of lenvatinib plus everolimus in human RCC xenograft models.** We next investigated the inhibitory effects of lenvatinib, everolimus, and the combination on tumor angiogenesis in A-498 and Caki-1 models, in which the combination treatment had induced tumor regression. Tumor angiogenesis was evaluated by measuring MVD after staining with an anti-CD31 antibody. Whereas lenvatinib monotherapy robustly reduced the MVD in A-498 xenografts, everolimus monotherapy did not (Fig. 2a, upper panels; Fig. 2b, left panel). In addition, MVD of mice bearing A-498 xenografts who received the lenvatinib plus everolimus combination treatment was equivalent to that in mice treated with lenvatinib monotherapy (Fig. 2a, upper panels; Fig. 2b, left panel), suggesting that angiogenesis was suppressed primarily by lenvatinib. This result was supported by data from the gene expression analysis, in which angiogenesis-related mouse genes were mainly downregulated by lenvatinib monotherapy and the combination treatment in A-498 xenografts (Fig. S1). Furthermore, the lenvatinib-induced anti-angiogenic effect in A-498 xenografts was associated with tissue hypoxia (Fig. S2). In the Caki-1 model, either lenvatinib or everolimus monotherapy significantly reduced MVD

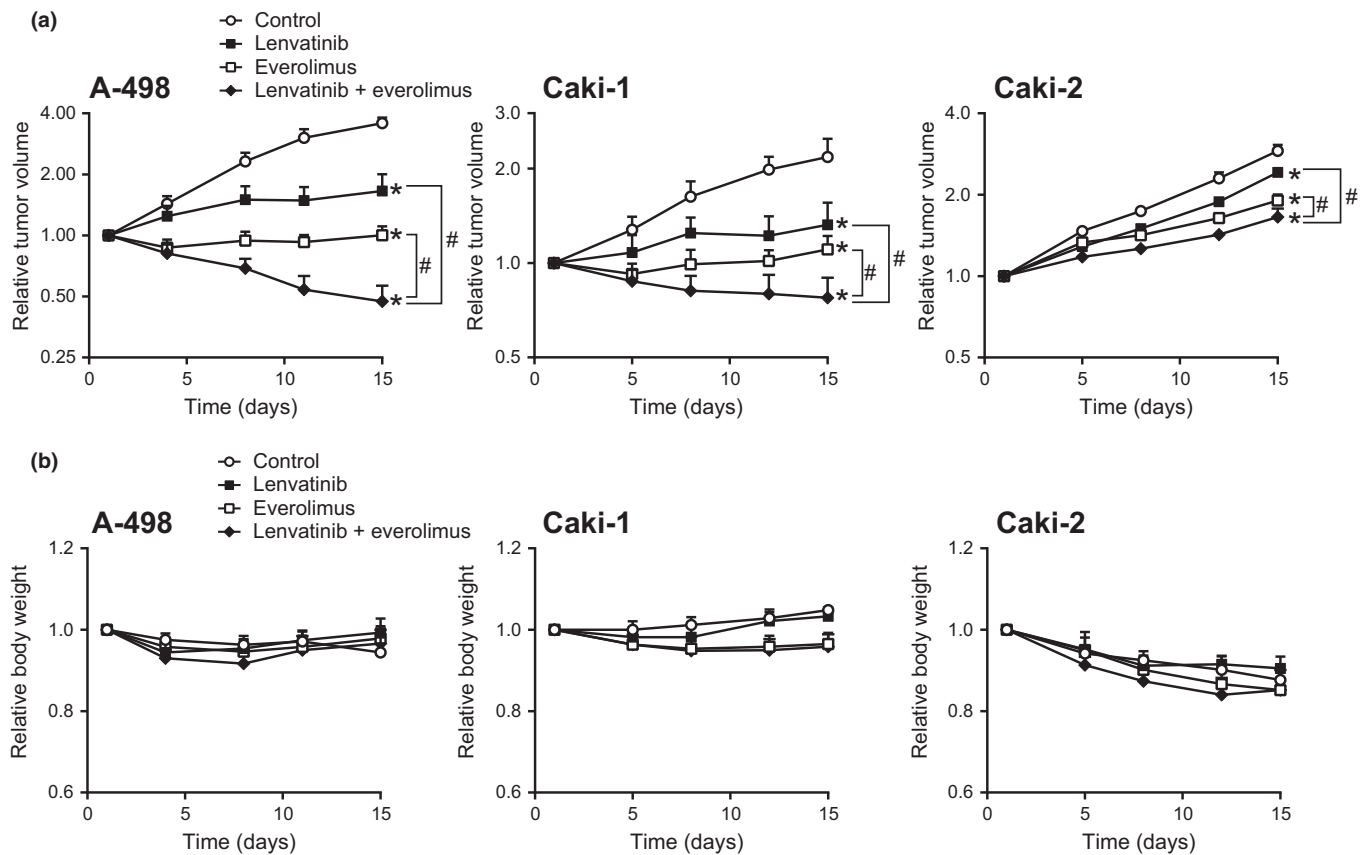


**Fig. 1.** Antitumor activities of lenvatinib, everolimus, and the lenvatinib plus everolimus combination in human renal cell carcinoma A-498, Caki-1, and Caki-2 xenograft models in mice. Mice orally received vehicle only, 10 mg/kg lenvatinib, 30 mg/kg everolimus, or both once daily for 14 days. (a) Relative tumor volume of A-498, Caki-1, or Caki-2 xenografts. Data on a log<sub>2</sub> scale are shown as mean + SD compared with tumor volume on day 1. \**P* < 0.05 versus vehicle control; #*P* < 0.05 between indicated treatments; *n* = 6 (Caki-1 and Caki-2) or 10 (A-498) mice per group. (b) Relative body weight of the same mice shown in (a). Data are expressed as mean + SD.

compared with the control, and the combination of lenvatinib plus everolimus achieved a greater decrease in MVD than either monotherapy (Fig. 2a, lower panels; Fig. 2b, right panel).

**Antiproliferative activity of lenvatinib and everolimus in A-498 and Caki-1 cells.** To examine whether lenvatinib and everolimus have an antiproliferative activity against A-498 and Caki-1 cells, we undertook *in vitro* proliferation assays. Cells were exposed to each drug for 6 days and then the relative number of viable cells was determined. The IC<sub>50</sub> values of everolimus in A-498 and Caki-1 cells were 5.46 nmol/L (95% confidence interval, 1.73–17.2) and 21.0 nmol/L (95% confidence interval, 4.34–102), respectively, whereas the IC<sub>50</sub> values of lenvatinib were >5 μmol/L in both cell lines. These findings indicate that everolimus (but not lenvatinib) potently inhibits the proliferation of these RCC cell lines. The antiproliferative effect of everolimus observed *in vitro* was consistent with the data that cell cycle-related genes were downregulated by everolimus monotherapy in A-498 xenograft model (Fig. S1).

**Effects of lenvatinib plus everolimus on VEGF-induced intracellular signaling and cell proliferation in HUVECs *in vitro*.** We then investigated the effects of combined treatment with lenvatinib plus everolimus on VEGF-stimulated cellular functions in endothelial cells *in vitro*. To clarify the effect of these compounds on intracellular signal transduction, we carried out Western blot analyses to assess the activities of Erk1/2, S6K, and S6. As expected, lenvatinib inhibited the phosphorylation of Erk1/2, S6K (Thr389 and Thr421/Ser424), and S6 (Ser235/

Ser236) through its inhibitory activity against VEGFR (Fig. 3a).<sup>(6)</sup> In contrast, everolimus suppressed the phosphorylation of S6K (Thr389 and Thr421/Ser424) and S6 (Ser235/Ser236), but not Erk1/2 (Fig. 3a). The combination of lenvatinib plus everolimus suppressed both the MAPK and mTOR pathways. Notably, the suppression of S6K (Thr421/Ser424) and S6 (Ser235/Ser236) phosphorylation was greater with the combination treatment than with either monotherapy (Fig. 3a). The apparent inability of the lenvatinib plus everolimus combination to enhance the inhibition of S6K (Thr389) phosphorylation probably reflects complete suppression by treatment with everolimus monotherapy.

Next, we used the median-effect method to evaluate the combined effects of lenvatinib plus everolimus on VEGF-driven proliferation of HUVECs. All treatments inhibited the VEGF-induced proliferation of HUVECs in a dose-dependent manner. The CI values for four dose ratios (lenvatinib:everolimus, 2.5:1, 5:1, 10:1, and 20:1) were between 0.80 and 1.17, indicating that the combination treatment resulted in mostly additive interactions (Table 1a).

**Effects of lenvatinib plus everolimus on FGF-induced intracellular signaling pathways and tube formation of HUVECs *in vitro*.** Fibroblast growth factor is another potent pro-angiogenic factor associated with tumor growth, including in RCC,<sup>(26,27)</sup> and we found that FGF was expressed in the three RCC cell lines we examined (Fig. S3). As lenvatinib inhibits both VEGF- and FGF-induced angiogenesis *in vivo*,<sup>(6)</sup> we assessed the effect of the lenvatinib plus everolimus



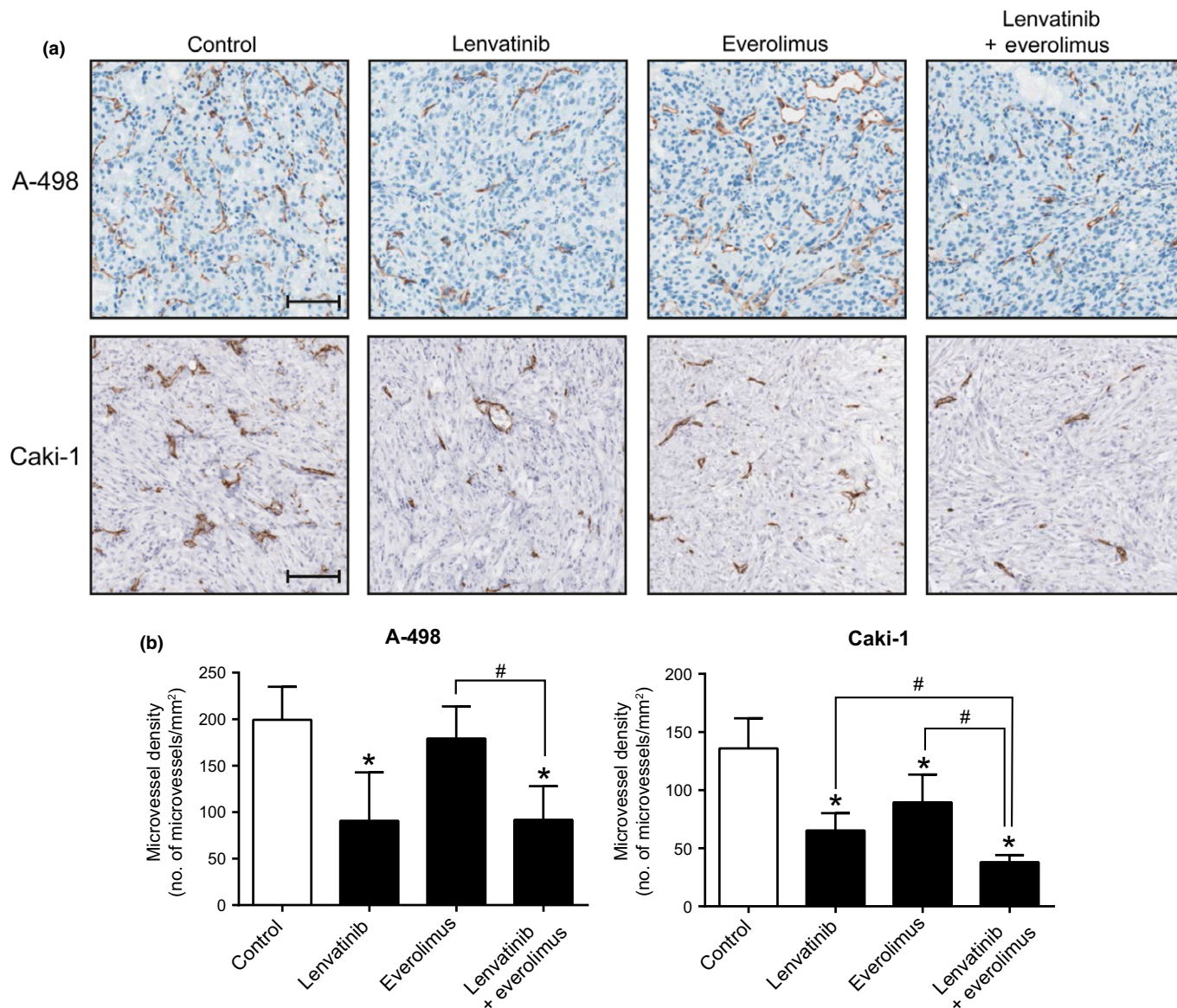


**Fig. 2.** Anti-angiogenic activity of lenvatinib, everolimus, and the lenvatinib plus everolimus combination in A-498 and Caki-1 renal cell carcinoma xenograft models. Mice bearing xenografts were randomly allocated to treatment groups when the tumor size had reached approximately 400–500 mm<sup>3</sup> (day1); mice then orally received vehicle only, 10 mg/kg lenvatinib, 30 mg/kg everolimus, or both once daily for 7 days. (a) Representative images of tumor microvessels stained by anti-CD31 antibody. For controls, vehicle-treated or untreated mice were used in the A-498 or Caki-1 model, respectively. Bar = 100 μm. (b) Effects on tumor microvessel density (MVD). Data are presented as mean + SD (*n* = 5 mice per group). \*MVD significantly (*P* < 0.05) different from control; #MVD significantly (*P* < 0.05) different between indicated treatments.

combination on FGF-induced angiogenesis. Similar to the effects on VEGF-stimulated signaling pathways in HUVECs, Western blot analyses showed that lenvatinib monotherapy suppressed both the MAPK and mTOR pathways in bFGF-stimulated HUVECs, whereas everolimus monotherapy inhibited only the mTOR pathway (Fig. 3b). However, S6K (Thr421/Ser424) and S6 (Ser235/Ser236) phosphorylation were inhibited more strongly by the lenvatinib plus everolimus combination than by either drug alone (Fig. 3b).

Combination index values from bFGF-induced tube formation assays were determined. In these experiments, drug effects on the ability of HUVECs (in response to bFGF) to form capillary-like structures on a gel containing basement membrane extract were examined.<sup>(28)</sup> Lenvatinib, everolimus, and the combination dose-dependently inhibited tube formation, and

the inhibitory effect of the combination treatment was greater than that of each monotherapy. The CI values for four dose ratios (lenvatinib:everolimus, 1:4, 1:8, 1:12, and 1:16) were between 0.47 and 0.74, indicating that this was mostly a synergistic interaction (Table 1b).

**Antitumor and anti-angiogenic activities of FGFR inhibitor in the Caki-1 xenograft RCC mouse model.** In MVD assays of Caki-1 xenograft mouse models, the combination of lenvatinib plus everolimus enhanced the anti-angiogenic effect (Fig. 2); therefore, we tested if FGF signaling influenced tumor growth and angiogenesis in this model using PD173074, an FGFR-selective inhibitor.<sup>(29)</sup> Tumor volume on day 15 after PD173074 (50 mg/kg) treatment was significantly smaller than control (Fig. 3c). In addition, MVD was also decreased after PD173074 treatment compared with vehicle control (Fig. 3d).

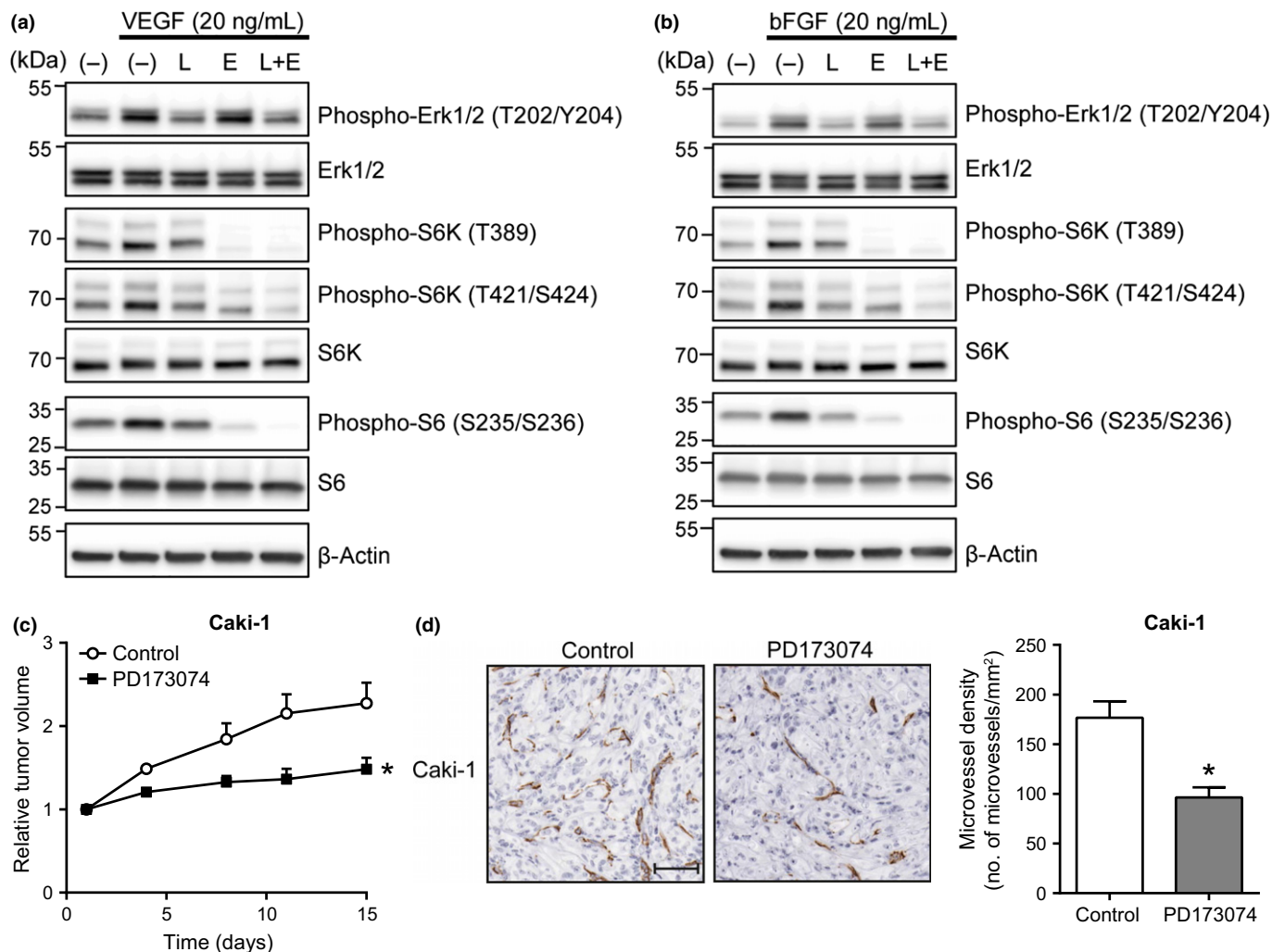


**Fig. 3.** Effects on vascular endothelial growth factor (VEGF)- or basic fibroblast growth factor (bFGF)-stimulated intracellular signaling, and FGF-induced angiogenesis and tumor growth. (a,b) Western blot analysis of phosphorylated (Phospho-) Erk1/2, S6K, and S6. Images shown are representative of three independent experiments. (a) VEGF-induced phosphorylation. HUVECs were treated for 1 h with vehicle only (-), 100 nmol/L lenvatinib (L), 1 nmol/L everolimus (E), or both, then stimulated with 20 ng/mL VEGF for 30 min. (b) bFGF-induced phosphorylation. HUVECs were treated for 1 h with vehicle only (-), 1000 nmol/L lenvatinib, 1 nmol/L everolimus, or both, then stimulated with 20 ng/mL bFGF for 30 min. (c) Antitumor activity of PD173074. Mice bearing Caki-1 xenograft tumors were randomly allocated to groups when their tumor size had reached approximately 400 mm<sup>3</sup> (day 1); mice then orally received 50 mg/kg PD173074 once daily for 14 days. Data are shown as RTV (mean + SD; n = 6 mice per group); \*P < 0.05 versus untreated control. (d) Anti-angiogenic activity of PD173074. Mice bearing Caki-1 xenograft tumors were randomly allocated to groups when their tumor size had reached approximately 500 mm<sup>3</sup> (day 1); mice then orally received 50 mg/kg PD173074 once daily for 14 days. Representative images of anti-CD31-positive tumor microvessels (left), and quantification of microvessel density on day 15 (right). Bar = 100 μm. Data are presented as mean + SD (n = 5 mice per group). \*P < 0.05 versus untreated control.

Taken together, these results indicate that FGF-driven tumor angiogenesis may contribute to Caki-1 tumor growth.

**Effects of lenvatinib, everolimus, and lenvatinib plus everolimus on VEGF- or FGF-driven angiogenesis-dependent tumor growth in mice.** Lenvatinib plus everolimus showed additive to synergistic inhibition of VEGF- or FGF-induced proliferation and tube formation of HUVECs *in vitro* (Table 1). To further examine these effects *in vivo*, we used KP-1 transfectant mouse models where tumor growths are supported by VEGF- or FGF-induced angiogenesis.<sup>(6)</sup> KP-1 transfectants were inoculated s.c. into mice, and when their tumor size had reached approximately 300 mm<sup>3</sup> (day 1), mice in each xenograft model were randomly allocated to six groups per xenograft model. Mice then received lenvatinib monotherapy, everolimus monotherapy, or the combination daily for 14 (KP-1/VEGF) or 10 (KP-1/FGF) days. Lenvatinib monotherapy at 7.5 mg/kg and everolimus monotherapy at 15 mg/kg significantly

inhibited tumor growth compared with vehicle control in both models (Fig. 4). Moreover, the combination treatment with lenvatinib (7.5 mg/kg) plus everolimus (15 mg/kg) showed significantly greater antitumor activity compared with either monotherapy at both identical and higher doses (Fig. 4). As with the RCC xenograft mouse models, the combination treatments were well tolerated, and did not cause greater body weight loss than either monotherapy (Fig. S4). These results indicate that combined treatment with lenvatinib plus everolimus exerts enhanced antitumor activity against tumor growth that is dependent on VEGF- or FGF-induced angiogenesis.

## Discussion

We showed here that the combination of lenvatinib plus everolimus exerted greater antitumor activity than either monotherapy in three human RCC xenograft mouse models. Furthermore,

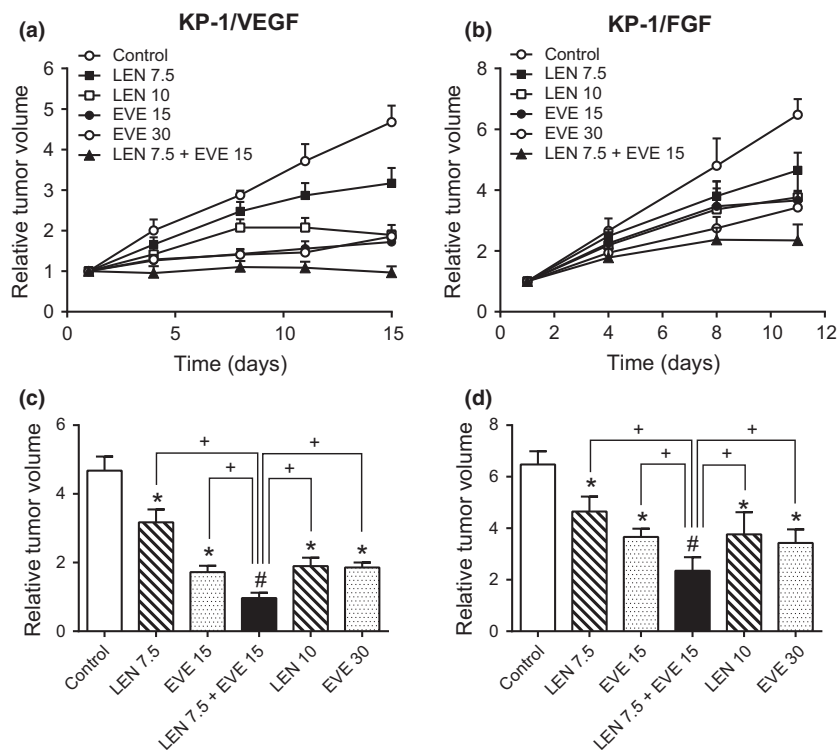


**Fig. 4.** Antitumor activity of lenvatinib (LEN), everolimus (EVE), and the combination of lenvatinib plus everolimus in KP-1/vascular endothelial growth factor (VEGF) and KP-1/fibroblast growth factor (FGF) xenografts in mice. Mice orally received vehicle only (control), lenvatinib (10 or 7.5 mg/kg), everolimus (30 or 15 mg/kg), or lenvatinib (7.5 mg/kg) plus everolimus (15 mg/kg) once daily for 14 days (KP-1/VEGF) or 10 days (KP-1/FGF). (a,b) Tumor growth of KP-1/VEGF (a) or KP-1/FGF (b) xenograft model (mean  $\pm$  SD;  $n = 5$  mice per group). (c,d) Enhanced antitumor activity of the combination of lenvatinib plus everolimus in KP-1/VEGF model on day 15 (c) or KP-1/FGF model on day 11 (d). \* $P < 0.05$  versus vehicle control;  $^{\dagger}P < 0.05$  between treatments;  $^{\#}P < 0.05$  versus vehicle control.

lenvatinib plus everolimus treatment led to tumor regression in two (A-498 and Caki-1) of the three models. The effects of the various treatments on tumor microvessels, however, differed between these two models: lenvatinib monotherapy was able to reduce MVD in both models, whereas everolimus monotherapy only resulted in decreased MVD in Caki-1 xenografts (Fig. 2). A combination effect on MVD was also noted only in this model (Fig. 2). In the Caki-1 model, therefore, the greater antitumor activity shown by the combination was a result of improved anti-angiogenic activity, whereas in the A-498 model, this appeared to be due to a combination of the anti-angiogenic activity of lenvatinib with the antiproliferative activity of everolimus. Our data indicated that the enhanced antitumor effect of lenvatinib plus everolimus in human RCC models is accomplished through two distinct mechanisms of action (Fig. 5a,b).

Mutation of the *VHL* gene is the most frequent genetic alteration in clear-cell RCC,<sup>(11)</sup> resulting in the induction of HIF-1 $\alpha$  and HIF-2 $\alpha$  even under normoxic conditions.<sup>(13)</sup> A-498 is a *VHL*-deficient RCC cell line, whereas Caki-1 is known to express wild-type *VHL*,<sup>(11,30)</sup> suggesting that lenvatinib can exert anti-angiogenic activity regardless of the *VHL* status. Although the combination effect on tumor angiogenesis was observed only in Caki-1 xenografts with wild-type *VHL*, we examined only a few cell lines in this study and therefore the relationship between *VHL* status and the combined anti-angiogenic activity warrants further investigation.

In Caki-2 xenograft model, we did not observe tumor regression even with the combination of lenvatinib plus everolimus (Fig. 1). It was reported that pericyte-covered vessels are relatively resistant to anti-angiogenic therapy,<sup>(31)</sup> and we previously reported that the

percentage of pericyte-covered vessels might predict lenvatinib activity in a panel of preclinical tumor xenograft models.<sup>(6)</sup> Caki-2 tumor tissues were relatively rich in stromal cells, which generally consist of cancer-associated fibroblasts and mural cells, and most of the microvessels were located in the stromal areas (data not shown). Thus, the tumor microenvironment status of Caki-2 xenografts might affect the sensitivity to lenvatinib, even when in combination with everolimus, and further investigations are required to elucidate the underlying mechanism.

Lenvatinib inhibits Erk1/2 and S6K-S6 signaling through blockade of VEGFR and FGFR (Fig. 5d).<sup>(6)</sup> In contrast, everolimus affects the mTOR pathway without influencing the phosphorylation of Erk1/2, but completely inhibits the phosphorylation of S6K (Thr389), which is predominantly phosphorylated by the mTOR complex.<sup>(32,33)</sup> However, the everolimus-inhibited phosphorylation of S6K (Thr421/Ser424) and S6 (Ser235/Ser236) was weaker than that of S6K (Thr389). In comparison, combined treatment with lenvatinib plus everolimus resulted in a much greater inhibition of the mTOR-S6K-S6 pathway, specifically of S6K (Thr421/Ser424) and S6 (Ser235/Ser236) phosphorylation. Previous reports have revealed that, downstream of the mTOR complex, S6K and S6 can also be activated by Erk1/2 signaling, with phosphorylation at the Thr421/Ser424 and Ser235/Ser236 residues, respectively (Fig. 5d).<sup>(32-34)</sup> Therefore, the greater inhibition of S6K and S6 may be due to lenvatinib blockade of Erk1/2 cross-signaling in the S6K-S6 pathway (downstream of mTOR), in addition to direct inhibition of mTOR by everolimus. Collectively, our results suggest that the inhibition of the MAPK pathway by lenvatinib and the increased inhibition of the



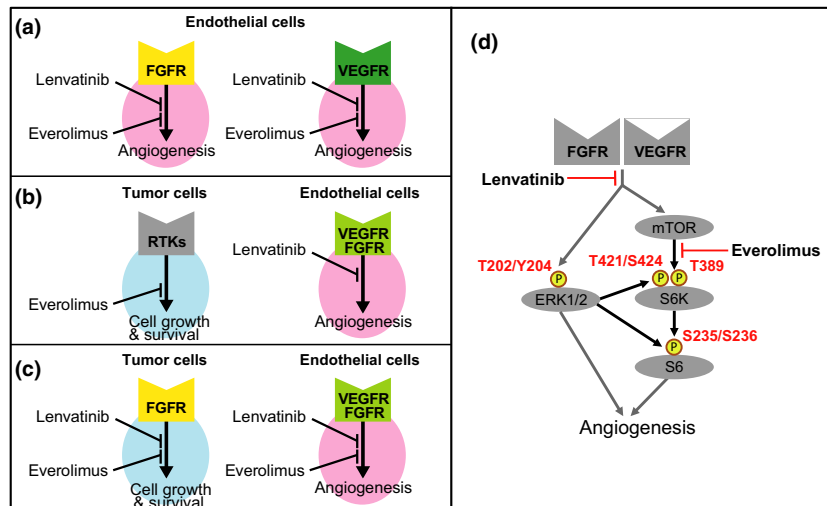


**Fig. 5.** Schematic models of multiple mechanisms of action underlying the antitumor activity of combined treatment with lenvatinib plus everolimus in renal cell carcinoma (RCC) xenograft mouse models. (a) Lenvatinib plus everolimus combination enhances the inhibition of both fibroblast growth factor (FGF)- and vascular endothelial growth factor (VEGF)-induced tumor angiogenesis (e.g. Caki-1 model). (b) Lenvatinib inhibits tumor angiogenesis and everolimus inhibits tumor cell proliferation, resulting in enhanced antitumor activity against RCC (e.g. A-498 model). (c) Lenvatinib and everolimus cooperate to enhance activity against RCC cell proliferation that is dependent on the FGF receptor (FGFR) signaling pathway. This model is hypothetical but is plausible in light of reports of the importance of the FGF pathway in RCC pathogenesis. (d) Mechanistic model of the dual inhibition of VEGF receptor (VEGFR)/FGFR and downstream mTOR signaling pathway. The increased inhibition of phosphorylation at S6K (T421/S424) and S6 (S235/S236) due to combined treatment with lenvatinib plus everolimus may result from the dual inhibition of both the Erk1/2 and mammalian target of rapamycin (mTOR) signaling pathways. RTK, receptor tyrosine kinase.

mTOR–S6K–S6 pathway by lenvatinib plus everolimus enhance the inhibitory effect of the drug combination on VEGF- and FGF-driven angiogenesis.

Accumulating evidence indicates that FGF acts as pro-angiogenic factor and that activation of the FGF signaling pathway is a potential mechanism of escape from anti-VEGF therapy, including in mRCC.<sup>(26,27)</sup> Given that: (i) FGF-mediated angiogenesis appears to play a major role in tumor growth in Caki-1 xenograft models (Fig. 3c,d); (ii) lenvatinib plus everolimus treatment resulted in tumor regression in this model (Fig. 1a); and (iii) lenvatinib is a strong inhibitor of FGF signaling,<sup>(6)</sup> we hypothesize that the tumor regression in Caki-1 xenograft mouse models by the lenvatinib plus everolimus combination is at least partly mediated through inhibition of FGF-mediated angiogenesis. The distinctive kinase inhibition profile of lenvatinib, specifically its inhibitory activity against FGFRs, may enable it to overcome FGF-mediated escape mechanisms from VEGF signaling inhibition, and likely, at least partially, underlies the clinical efficacy of the combination of lenvatinib plus everolimus seen in patients with mRCC. Both FGFR1 and FGFR2 are over-expressed in mRCC, and FGF signaling in RCC tumor cells is also associated with malignancy and intrinsic resistance to VEGFR inhibition.<sup>(35–37)</sup> The combined targeting of the FGFR and mTOR pathways in RCC tumor cells may also be another mechanism underlying the observed clinical activity of the lenvatinib plus everolimus combination (Fig. 5c). However, as IC<sub>50</sub> values of lenvatinib in A-498 and Caki-1 cell proliferation assays exceeded 5 μmol/L, we surmised that lenvatinib lacked direct antiproliferative activity in these cells. Further experiments using RCC cell lines highly addicted to FGF signaling and tumor tissue samples from patients with RCC who are resistant to VEGF-targeted agents may yield additional insight into the potent antitumor activity of the lenvatinib plus everolimus combination.

In summary, we propose a plausible biologic rationale for the observed antitumor activity of the lenvatinib plus everolimus

combination in preclinical RCC models. We postulate that the enhanced activity of this combination treatment is due to the following activities of the two individual compounds: (i) lenvatinib and everolimus additively or synergistically inhibit FGF- as well as VEGF-induced angiogenesis (Fig. 5a); (ii) lenvatinib has potent anti-angiogenic activity, whereas everolimus exerts a direct antitumor effect (Fig. 5b); and (iii) lenvatinib and everolimus cooperate in the inhibition of FGF-driven tumor growth (Fig. 5c). Targeting multiple oncogenic pathways by using combinations of molecularly targeted agents can enhance the efficacy of, or overcome the resistance associated with, monotherapies. We showed here that the combination of lenvatinib plus everolimus targets both tumor cell growth and angiogenesis. Therefore, combination treatment with agents that individually target tumor cells as well as non-tumor cells that contribute to the tumor microenvironment may be a powerful and promising concept for potent tumor suppression.

## Disclosure Statement

All authors are employees of Eisai Co., Ltd.

## Abbreviations

bFGF	basic fibroblast growth factor
CI	combination index
FGF	fibroblast growth factor
FGFR	fibroblast growth factor receptor
HIF	hypoxia-inducible factor
mRCC	metastatic renal cell carcinoma
mTOR	mammalian target of rapamycin
MVD	microvessel density
p/s	100 units/mL penicillin–100 μg/mL streptomycin
RCC	renal cell carcinoma
RTV	relative tumor volume
VEGF	vascular endothelial growth factor
VEGFR	vascular endothelial growth factor receptor
VHL	von Hippel–Lindau



## References

- Schlumberger M, Tahara M, Wirth LJ, *et al.* Lenvatinib versus placebo in radioiodine-refractory thyroid cancer. *N Engl J Med* 2015; **372**: 621–30.
- Matsui J, Yamamoto Y, Funahashi Y, *et al.* E7080, a novel inhibitor that targets multiple kinases, has potent antitumor activities against stem cell factor producing human small cell lung cancer H146, based on angiogenesis inhibition. *Int J Cancer* 2008; **122**: 664–71.
- Matsui J, Funahashi Y, Uenaka T, Watanabe T, Tsuruoka A, Asada M. Multi-kinase inhibitor E7080 suppresses lymph node and lung metastases of human mammary breast tumor MDA-MB-231 via inhibition of vascular endothelial growth factor-receptor (VEGF-R) 2 and VEGF-R3 kinase. *Clin Cancer Res* 2008; **14**: 5459–65.
- Okamoto K, Kodama K, Takama K, *et al.* Antitumor activities of the targeted multi-tyrosine kinase inhibitor lenvatinib (E7080) against RET gene fusion-driven tumor models. *Cancer Lett* 2013; **340**: 97–103.
- Tohyama O, Matsui J, Kodama K, *et al.* Antitumor activity of lenvatinib (E7080): an angiogenesis inhibitor that targets multiple receptor tyrosine kinases in preclinical human thyroid cancer models. *J Thyroid Res* 2014; **2014**: 638747.
- Yamamoto Y, Matsui J, Matsushima T, *et al.* Lenvatinib, an angiogenesis inhibitor targeting VEGFR/FGFR, shows broad antitumor activity in human tumor xenograft models associated with microvessel density and pericyte coverage. *Vasc Cell* 2014; **6**: 18.
- Yamada K, Yamamoto N, Yamada Y, *et al.* Phase I dose-escalation study and biomarker analysis of E7080 in patients with advanced solid tumors. *Clin Cancer Res* 2011; **17**: 2528–37.
- Boss DS, Glen H, Beijnen JH, *et al.* A phase I study of E7080, a multitargeted tyrosine kinase inhibitor, in patients with advanced solid tumours. *Br J Cancer* 2012; **106**: 1598–604.
- Gupta K, Miller JD, Li JZ, Russell MW, Charbonneau C. Epidemiologic and socioeconomic burden of metastatic renal cell carcinoma (mRCC): a literature review. *Cancer Treat Rev* 2008; **34**: 193–205.
- Fisher R, Gore M, Larkin J. Current and future systemic treatments for renal cell carcinoma. *Semin Cancer Biol* 2013; **23**: 38–45.
- Gnarra JR, Tory K, Weng Y, *et al.* Mutations of the VHL tumour suppressor gene in renal carcinoma. *Nat Genet* 1994; **7**: 85–90.
- Whaley JM, Naglich J, Gelbert L, *et al.* Germ-line mutations in the von Hippel-Lindau tumor-suppressor gene are similar to somatic von Hippel-Lindau aberrations in sporadic renal cell carcinoma. *Am J Hum Genet* 1994; **55**: 1092–102.
- Krieg M, Haas R, Brauch H, Acker T, Flamme I, Plate KH. Up-regulation of hypoxia-inducible factors HIF-1 $\alpha$  and HIF-2 $\alpha$  under normoxic conditions in renal carcinoma cells by von Hippel-Lindau tumor suppressor gene loss of function. *Oncogene* 2000; **19**: 5435–43.
- Gunningham SP, Currie MJ, Han C, *et al.* Vascular endothelial growth factor-B and vascular endothelial growth factor-C expression in renal cell carcinomas: regulation by the von Hippel-Lindau gene and hypoxia. *Cancer Res* 2001; **61**: 3206–11.
- Wiesener MS, Munchenhagen PM, Berger I, *et al.* Constitutive activation of hypoxia-inducible genes related to overexpression of hypoxia-inducible factor-1 $\alpha$  in clear cell renal carcinomas. *Cancer Res* 2001; **61**: 5215–22.
- Motzer RJ, Jonasch E, Agarwal N, *et al.* Kidney cancer, version 3.2015. *J Natl Compr Canc Netw* 2015; **13**: 151–9.
- Pantuck AJ, Seligson DB, Klatte T, *et al.* Prognostic relevance of the mTOR pathway in renal cell carcinoma: implications for molecular patient selection for targeted therapy. *Cancer* 2007; **109**: 2257–67.
- Robb VA, Karbowiczek M, Klein-Szanto AJ, Henske EP. Activation of the mTOR signaling pathway in renal clear cell carcinoma. *J Urol* 2007; **177**: 346–52.
- Lane HA, Wood JM, McSheehy PM, *et al.* mTOR inhibitor RAD001 (everolimus) has antiangiogenic/vascular properties distinct from a VEGFR tyrosine kinase inhibitor. *Clin Cancer Res* 2009; **15**: 1612–22.
- Boulay A, Lane HA. The mammalian target of rapamycin kinase and tumor growth inhibition. *Recent Results Cancer Res* 2007; **172**: 99–124.
- Siegel RL, Miller KD, Jemal A. Cancer statistics, 2016. *CA Cancer J Clin* 2016; **66**: 7–30.
- Michaelson MD. Combination of targeted agents in metastatic renal cell carcinoma: a path forward or a dead-end street? *Cancer* 2012; **118**: 1744–6.
- Motzer RJ, Hutson TE, Glen H, *et al.* Lenvatinib, everolimus, and the combination in patients with metastatic renal cell carcinoma: a randomised, phase 2, open-label, multicentre trial. *Lancet Oncol* 2015; **16**: 1473–82.
- Chou TC, Talalay P. Quantitative analysis of dose-effect relationships: the combined effects of multiple drugs or enzyme inhibitors. *Adv Enzyme Regul* 1984; **22**: 27–55.
- Chou TC. Theoretical basis, experimental design, and computerized simulation of synergism and antagonism in drug combination studies. *Pharmacol Rev* 2006; **58**: 621–81.
- Rini BI, Atkins MB. Resistance to targeted therapy in renal-cell carcinoma. *Lancet Oncol* 2009; **10**: 992–1000.
- Weldt JC, Gourlaouen M, Powles T, *et al.* Fibroblast growth factor 2 regulates endothelial cell sensitivity to sunitinib. *Oncogene* 2011; **30**: 1183–93.
- Ichikawa K, Watanabe-Miyano S, Adachi Y, Matsuki M, Okamoto K, Matsui J. Lenvatinib suppresses angiogenesis through the inhibition of both the VEGFR and FGFR signaling pathways. *Glob J Cancer Ther* 2016; **2**: 019–25.
- Pardo OE, Latigo J, Jeffery RE, *et al.* The fibroblast growth factor receptor inhibitor PD173074 blocks small cell lung cancer growth in vitro and in vivo. *Cancer Res* 2009; **69**: 8645–51.
- Maxwell PH, Wiesener MS, Chang GW, *et al.* The tumour suppressor protein VHL targets hypoxia-inducible factors for oxygen-dependent proteolysis. *Nature* 1999; **399**: 271–5.
- Bergers G, Hanahan D. Modes of resistance to anti-angiogenic therapy. *Nat Rev Cancer* 2008; **8**: 592–603.
- Iijima Y, Laser M, Shiraiishi H, *et al.* c-Raf/MEK/ERK pathway controls protein kinase C-mediated p70S6K activation in adult cardiac muscle cells. *J Biol Chem* 2002; **277**: 23065–75.
- Lehman JA, Calvo V, Gomez-Cambronero J. Mechanism of ribosomal p70S6 kinase activation by granulocyte macrophage colony-stimulating factor in neutrophils: cooperation of a MEK-related, THR421/SER424 kinase and a rapamycin-sensitive, m-TOR-related THR389 kinase. *J Biol Chem* 2003; **278**: 28130–8.
- Roux PP, Shahbazian D, Vu H, *et al.* RAS/ERK signaling promotes site-specific ribosomal protein S6 phosphorylation via RSK and stimulates cap-dependent translation. *J Biol Chem* 2007; **282**: 14056–64.
- Tsimafeyeu I, Demidov L, Stepanova E, Wynn N, Ta H. Overexpression of fibroblast growth factor receptors FGFR1 and FGFR2 in renal cell carcinoma. *Scand J Urol Nephrol* 2011; **45**: 190–5.
- Ho TH, Liu XD, Huang Y, *et al.* The impact of FGFR1 and FRS2 $\alpha$  expression on sorafenib treatment in metastatic renal cell carcinoma. *BMC Cancer* 2015; **15**: 304.
- Tsimafeyeu I, Bratslavsky G. Fibroblast growth factor receptor 1 as a target for the therapy of renal cell carcinoma. *Oncology* 2015; **88**: 321–31.

## Supporting Information

Additional Supporting Information may be found online in the supporting information tab for this article:

**Fig. S1.** Effects of lenvatinib, everolimus, and the combination on gene expressions in A-498 renal cell carcinoma xenografts.

**Fig. S2.** Tissue hypoxia in A-498 renal cell carcinoma xenografts.

**Fig. S3.** Expression levels of *VEGFA*, *FGF1*, *FGF2* (basic FGF), and *MTOR* in A-498, Caki-1, and Caki-2 renal cell carcinoma cells *in vitro*.

**Fig. S4.** Relative body weight in KP-1/vascular endothelial growth factor (VEGF) and KP-1/fibroblast growth factor (FGF) xenograft models.

**Table S1.** TaqMan gene expression assays used for quantitative RT-PCR analysis.

**Appendix. S1.** Supporting materials and methods.